4

Characterization Methods and Techniques

Noppadon Sathitsuksanoh[1] *and Scott Renneckar*[2]

[1] *University of Louisville, Department of Chemical Engineering, Louisville, KY, USA*
[2] *Virginia Tech, Department of Sustainable Biomaterials, Blacksburg, VA, USA*

4.1 Philosophy Statement

Humans are entering a new age when we can have significant control over the genomic make-up of plants and organisms that can operate on biomass. Understanding physiochemical characteristics of plant biomass helps us in the upstream and downstream processes. In the upstream process, information of plant biomass' characteristics aids in engineering them to have desirable traits including drought resistance or *in planta* production of metabolites such as cancer drugs. For downstream process, the characteristic information of plant biomass aids us in designing the pathways to break and transform them into valuable products. Herein, we learn what information these selected characterization methods and techniques for plant biomass provide and how to interpret and use those information.

4.2 Understanding the Characteristics of Biomass

Plants contain stored solar energy in the form of glucose that is transformed into a host of other compounds and materials such as polysaccharides, lipids, and lignins. Glucose is used to power cell metabolism and is the precursor for the structural polymers of the plant wall. The simplicity of the ingredients in photosynthesis of water and carbon dioxide results in the plant consisting of the primary elements of carbon, hydrogen, and oxygen; however, plants also require nitrogen and sulfur and other trace elements such as calcium and potassium. Nitrogen and sulfur are necessary for the formation of proteins that encode the life of the plant, while the metals form ions that assist in membrane transport and catalytic sites in cellular enzymes. During the growth of the plant, these compounds are woven into the complex tapestry of the biomass cell wall and this chapter explores methods to characterize this complex material.

Although the compounds in the cell wall start out as a simple carbohydrate of glucose, this is only a building block that is modified, polymerized, and transformed into the structural polymers that support the plant. Additional extraneous materials are formed that lend the plant defense against attacking organisms, such as terpenoids,

Introduction to Renewable Biomaterials: First Principles and Concepts, First Edition.
Edited by Ali S. Ayoub and Lucian A. Lucia.

tannins, and other reserve materials that are inside the cell lumen, cell microfissures, and intercellular space such as resin canals. These materials are typically classified as extractives because they can be readily removed through the process of soaking the biomass in solvents with various solubility parameters that remove the compounds into the solvent. This simple extraction method is similar to the process of making a cup of coffee. It is an example of diffusion where the extractive compounds move from an area of high concentration, the cell wall, into an area of low concentration, the solvent. Depending upon the species of the plant, the location of the tissue that is being sampled within the plant, as well as the location of where it was grown there is variability of the amount of extractive content from less than a percent by weight of the mass to over 10% in some species like the heartwood of redwood [1].

Lastly, biomass has varying levels of water associated with it. Water can be tightly associated with the cell wall through hydrogen bonding to the structural framework. Because of the close association of the water, this water is usually known as bound water and has properties that are different from water that is free to associate with itself in liquid form, free water. The biomass has a limit of interaction sites, and once those spaces are occupied, any excess water is found in the cell lumen as free water. This free water can be physically squeezed out of biomass. The importance of understanding the moisture content of the biomass lies in the fact that analysis of biomass requires a known plant or biopolymer dry mass; any unaccounted moisture can cause a miscalculation of the composition or polymer size. Hence, when investigating biomass or biopolymers the amount of moisture must be first determined for the sample.

4.3 Taking Precautions Prior to Setting Up Experiments for Biomass Analysis

Before we move into the analysis of biomass using specific techniques and characterization methods, a point of caution must be made about the reliability of the analyzed data, in relation to the scientist's goals and the error that can be introduced during the evaluation of the material. Biomass is variable from species to species, plant to plant within a species, and location to location within the plant. All of the variability is dependent on a number of genetic and environmental cues, both nature and nurture! While scientists can have controlled studies where there is a comparison of two groups, by knocking out or inserting genes, or purposely changing nutrient and growing conditions of plants, it should be cautioned that samples must be representative of the study's objectives. Hence, investigating the intrinsic properties of the plant requires a wide sampling range of the biomass from the field or forest. In contrast, if the impact of a processing technique is to be measured, then most likely a narrow sampling range can help pinpoint the changes caused by processing. In both cases, a rigorous study requires that enough sample is analyzed so the investigator is confident in the data and that the results are statistically representative of the population. To do this experimental work, randomized replications are made and the variation of the results is used to understand the validity of the average.

A common issue that is found with novice experimentalists is that often replications are only made of the measurement and not the variable being investigated. Hence, when designing experimental testing protocols, the objective is to replicate the variable of

interest and not necessarily the accuracy of the measurement method. The researcher should already have an idea of the degree of variability, or accuracy, of the measurement, and they should take that into account during analysis. For example, if the moisture content of a sample is being determined using gravimetric methods, the researcher should know the limit of error of the balance and should not take the same sample and weigh it three times after drying it to produce an average of the mass. This result would provide only information about the variability of the measurement and would not provide an insight into the variability of the moisture content of the biomass.

Review questions:

1. Name three classes of *nonstructural* components that are involved in the cell wall composition.
2. How could moisture content vary across an open container of wood particles?
3. Describe the impact of error of a noncalibrated balance, the error related to the resolution of the balance, and error related to copying the wrong information into their lab notebook in relation to the accuracy of the data.

4.4 Classifying Biomass Sizes for Proper Analysis

For most analytical experiments biomass samples are resized into smaller particles that range from single-digit millimeters down to single-digit micrometers depending upon the specifications of the analytical method. Various grinders and mills can be used to resize biomass ranging from a simple coffee bean grinder, available at home stores, to screened knife mills designed to control the degree of particle breakdown. Most analytical standards provide guidance to the size of the particles desired for analysis. These particle sizes are based on screen size of which the particles pass through and occasionally the screen size that particles are retained. Resizing the particles helps with randomizing the biomass as it mingles together with samples from multiple plants or multiple areas of the stem, which is obviously dependent upon what is going into the grinder. If the particles are too large during the preparation of samples for analysis, then the mass transfer is slowed by the biomass anatomical structure and potential density variations across the sample. Only partial reactions occur in the allotted time of the standard if the appropriate particle size is not selected. On the other hand, if particles are too small, then particles can easily clog filters and form colloidal suspensions that are difficult to precipitate and recover for analysis.

As indicated later, knife-milled biomass of size 20–80 mesh is used in many analytical procedures as well as chemical reactions and modifications. Knife milling requires first the resizing of large biomass pieces to scale so that these pieces can be easily fed into the processing equipment. Screen selection should occur based on the requirements of the analytical procedure. Screens are delicate and with extended use can become damaged, so screens should be inspected periodically. Additionally, extremely wet biomass does not mill into a uniform product and readily clogs screens as the biomass is smeared instead of cut. On the other hand, not all knife mills can handle biomass and caution should be taken with extremely high-density biomass. The interior shell of a coconut is composed of lignocellulosic material and has a density well above

1000 kg m^{-3}, as a result the shell will dull knife blades quickly. Other screened mills like hammer mills are used to resize high-density biomass. This machinery strikes biomass with a group of rotating bars and the particles exit the equipment through a screen of specified size. Because of their simplicity, often these mills are used in industrial settings to resize biomass for feeding into furnaces. Both hammer and knife mills cause localized temperature increases of the biomass from frictional heating, free radical formation from chain cleavage, and the researcher should be aware of this potential for temperature-sensitive samples like cellulose [2].

After particles pass through a given screen size in a knife mill, there is a range of sizes that diminish into the size of an ultrafine powder. While not always required by the standard, a more uniform sample will lead to more reproducible results [3]. Milled samples can be placed in stacked screens to obtain particles of uniform size for characterization purposes. These screens have mechanical motors that shake material back and forth or have high-frequency vibrations to help move particles across and through the screens of select sizes. A caveat is given to the student – overloading the screens with biomass samples often will limit screening effectiveness.

Occasional analytical methods require extensive milling of the material using a planetary style ball mill [4]. Cups filled with resized biomass and ceramic balls of various sizes are rotated for extended time periods collapsing the particle microstructure and turning the wood into a fine powder; this fine structure would be like transforming sugar cubes into a fine powder such as confectioner's sugar. This transformation is important in studies using ionic liquids to dissolve whole biomass or methods to isolate certain components like lignin. The former allows the use of analytical experiments like 2D (two-dimensional) nuclear magnetic resonance (NMR) spectroscopy to identify molecular structure found in plant biomass without having to extract individual components. In contrast, isolation of individual components modifies the biopolymers because intermolecular linkages between lignin and carbohydrates require cleavage. To this end, research has been performed in an attempt to limit the degree of modification during isolation. Guerra *et al*. [5] developed a method of milling wood into a fine powder, enzymatically removing much of the polysaccharide component with cellulases, and then performing a mild acidolysis reaction to obtain a relatively unmodified lignin compared to technical lignins from pulping operations.

4.5 Moisture Content of Biomass and Importance of Drying Samples Prior to Analysis

An accurate moisture content must be determined for the analysis of biomass and biopolymers and, in most cases, the moisture should be removed. While this task is relatively simple, achieved by heating the biomass and determining the moisture content gravimetrically (measured through the change in mass), an important issue must be addressed. Not all volatile compounds that can be removed through heating are water molecules; certain extractives are removed through high-temperature oven drying. While many extractives are highly polar and are solid at elevated temperatures, there are certain terpenoids, such as α- and β-pinene, that have a boiling point near 155 °C. In these cases, industrial dryers may heat samples beyond the boiling point of these compounds.

Additionally, there are two methods to calculate the moisture content of the biomass. One method uses a ratio of the water to the dry mass of the plant material and because of this ratio, moisture contents can be greater than 100%. Typical tables listing the moisture content of green wood, wood that has never been dried, will use this calculation method. The other method describes the amount of water as a fraction of the total mass of the sample. This number is used when calculating the equivalent dry mass and is directly used in most calculations as percent solids or volatiles.

Common laboratory methods to determine the dry mass, known as "oven-dry mass" of the biomass utilize lyophilization, vacuum drying, convection oven drying, or fluid-bed dryers. The choice of the different methods depends upon the starting moisture content along with the sensitivity of the structure to thermal processing. Higher temperature oven drying can cause the collapse of the ultrafine biopolymer structure resulting in a change in crystallinity and reactivity of the sample. In the pulp and paper industry, this is referred to hornification where the cellulose structure is annealed into a highly packed state [6]. Lyophilization, often commonly referred to as freeze drying, provides a sample with a more open structure without the oven drying–induced changes. One example of the sensitivity of biomass structure to drying methods is seen through the difference in crystallinity index (CrI) of freeze-dried versus air-dried nanocellulose [7]. With freeze-drying suspensions of nanocellulose, there is some reaggregation of samples into films and fibers as demonstrated by Hsieh and coworkers [8]. Some of these changes can be reversible given the right methods of activation [9]. This reversibility of structure is illustrated by a using a solvent exchange process to remove the water from the reswollen fiber. Furthermore, to dissolve cellulose in nonderivatizing solvents like dimethyl acetamide (DMAc) LiCl solutions, cellulose dissolution requires activation by first swelling the cellulose in a water solution, then stepwise removing the water by using different concentrations of methanol and then exchanging the absolute for DMAc [10]. Dissolving cellulose is important for a variety of chemical characterization methods, especially related to molecular weight determination, which is discussed.

4.6 When the Carbon is Burned

Humans have been using biomass as bioenergy for millennia in the form wood-heated stoves. One of the primary uses of biomass for bioenergy is the use of pellets for the combustion to either generate electricity directly through steam turbines or through high-temperature gasification. Biomass pellets have the advantage of using modern day carbon. The drawback of using these materials is the ash particulates that impact emissions and furnace maintenance. Hence knowledge of the ash content is critical when using wood for bioenergy production. The benefit of the excess ash from an industrial conversion process is that much of this can be recovered and used as fertilizer.

Ash content is determined gravimetrically after the combustion of the biomass at high temperatures in a muffle furnace [11]. Ceramic-based crucibles are required for the combustion process along with desiccators to store the samples as they cool. Ash content is expressed as an overall percentage of the dry matter. In some cases, ash content can be as high as 1% in some wood species and even higher in tropical wood species. There are a variety of different levels of ash content depending upon the biomass type ranging from materials such as rice straw that contains significant amount of silica upward of

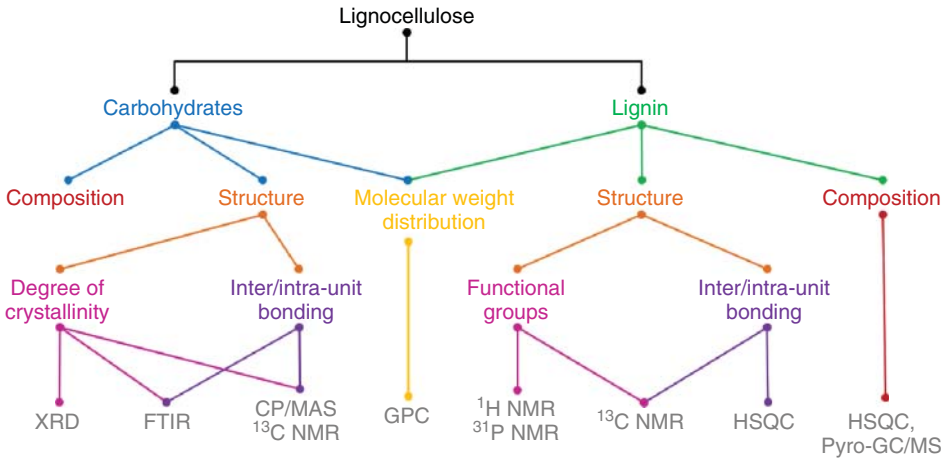

Figure 4.1 Biomass characterization diagram shows common characterization techniques for carbohydrates and lignin.

15% [12], to corn stover that is 6% [12], to some energy grasses such as switchgrass that has levels of 3–7% [12]. Mineral levels of ash do vary by stalk versus leaf material, as well as position in the stem and growing location of the plant. Another method to measure ash content is to use thermogravimetric analysis equipment, where the sample is heated on a balance pan to very high temperatures in an air environment. This method is essentially microsampling the material, as analysis is limited to 10–50 mg of material.

Figure 4.1 shows the diagram of common characterization techniques for lignocellulose. There are two major lignocellulosic components: (i) carbohydrates and (ii) lignin. Both carbohydrate and lignin can be characterized by various techniques to learn about their physiochemical characteristics. These information are useful in

- engineering plant biomass to have certain traits including (i) less recalcitrant and (ii) more drought resistant and/or
- designing biological and/or chemical pathways to degrade and/or convert plant biomass into valuable products.

4.7 Structural Cell Wall Analysis, What To Look For

The structural components of the cell wall of biomass are composed of a mixture of carbohydrates (i.e., polysaccharides) and lignin closely integrated within the cell wall. In order to fully utilize lignocellulose, robust analytical techniques for their quintessential traits (Table 4.1) are required for analysis. Changes in carbohydrate and lignin compositions, chemical structure, and functionality affect fiber properties and ultimately product quality.

Recent imaging studies of the cell wall provided insight into the arrangement of these compounds related to the biological synthesis of the cell wall [58]. Cellulose is deposited as bundles within the cell wall of various diameters, dependent upon the plant type, and their orientation controlled by microtubules. During deposition,

Table 4.1 Selected characterization methods of structural carbohydrates and lignin.

Biomass characteristics	Techniques
Composition of lignocellulose	• Two-step acid hydrolysis [11, 13, 14]
Monosaccharide and lignin contents	• High-pressure liquid chromatography (HPLC)
Degree of crystallinity Changes of inter-/intramolecular hydrogen bonding of polysaccharides	• Cross-polarization/magic angle spinning (CP/MAS) ^{13}C nuclear magnetic resonance (NMR) [15–17] • X-ray diffraction (XRD) [15–17] • Fourier-transform infrared (FTIR) (lateral order index (LOI)) [15–19]
p-Hydroxyphenyl (H): guaiacyl (G): syringyl (S) ratio	• FT-Raman [20–22] • Pyrolysis-gas chromatography/mass spectrometry (Pyro-GC/MS) [23–26] • 2D heteronuclear single-quantum correlation (HSQC) [27–31] • ^{13}C NMR [32, 33]
Hydroxyl functional groups of lignin	• Wet chemistries [34, 35] • ^{1}H NMR [34–38] • ^{13}C NMR [34, 36, 39] • ^{31}P NMR [34, 40–43] • FTIR [34, 35] • Ultraviolet (UV) spectroscopy [35–37]
Lignin structural information	• ^{13}C NMR [32, 44]
Structural types and distribution of interunit bonding patterns of lignin	• 2D HSQC [4, 45–48]
Molecular weight distribution	• Gel permeation chromatography (GPC) [49–52]
Degree of condensation of lignin	• Cross-polarization-polarization-inversion (CPPI) [53–55] • ^{13}C NMR [44, 56] • ^{31}P NMR [57]

there are heteropolysaccharides present that assemble onto the cellulose microfibril surfaces. There is a lack of any evidence for any covalent bonding between the cellulose and heteropolysaccharides, suggesting a physical association among the components. The heteropolysaccharides are thought to help space the microfibrils in the hydrogel-like network as the charged substituents like glucuronic acid give rise to longer distant repulsive forces [59]. At the end of the life of the vascular cell, monolignols are transported from the cytosol of the cell into the polysaccharide cell wall where they undergo dehydrogenative polymerization induced by a variety of protein-based enzymes. Side reactions occur during these processes linking lignin to the heteropolysaccharides, usually through benzyl ether linkages or gamma carbon esters of the propanol side chain [60].

By now it should be clear that the complex structure of the cell wall mandates careful analytical procedures to quantify the composition of the components that go into the cell wall. With an emphasis on the conversion and utilization of the polysaccharides, especially glucose, for liquid fuel production, it is important to know the amount of

cellulose in order to close the total mass balance. The simplest approach would be to separate each component and weigh out exactly how much is present. Since each component cannot be fully extracted in a stepwise, perfectly quantitative manner, biomass is treated with a mineral acid that cleaves the acetal linkages among the polysaccharides reducing the biomass into a soup containing monosaccharides and heavily modified lignin, along with a few degradation by-products such as furfural compounds. The majority of the lignin remains in particulate form and can be separated via filtration through a ceramic filter and the concentration of monosaccharides determined via chromatographically.

4.8 Hydrolyzing Biomass and Determining Its Composition

Compositional analysis is one of the most common ways to understand the chemical make-up of lignocellulose. Lignocellulose is a complex biopolymer of three major lignocellulose components: cellulose, lignin, and hemicelluloses. The latter is actually a collection of heteropolysaccharides that are composed of more than one monosaccharide. In order to quantify the amount of these components, lignocellulose is required to be hydrolyzed by two-step acid hydrolysis. The first step is to transform polymers into oligomers, followed by the second step to further hydrolyze oligomers to monomers [13]. The methods have been extensively developed by the National Renewable Energy Laboratory (NREL), and an overview is given in the following.

In a typical method, extractive free biomass [14] is first hydrolyzed with concentrated acid. The biomass is ground to 20–80 mesh size and 300 mg dry lignocellulose is mixed with 3 ml of 72% (w/w) sulfuric acid. This work can be conducted in a test tube incubated water bath maintained at 30 °C. The mixture is incubated for 1 h and can be stirred intermittently with a glass rod. After 1 h, the reaction mixture is diluted with water (~84 ml water) to a final concentration of 4% (w/w) sulfuric acid solution. Caution should be used when handling the acid and mixing with water. For the second step hydrolysis, the reaction mixture is transferred into pressurized reactor vessels (e.g., pressure tubes) and autoclaved at 121 °C (15 psi) for 1 h. These two steps will cause the polysaccharides to depolymerize, cleave the acetate groups from the hemicelluloses, and dissolve a small portion of the lignin, usually less than 2% as acid-soluble lignin (ASL). The ASL can be determined by spectrophotometer at $\lambda = 240$ and 320 nm, depending on the type of biomass species [13]. The lignin undergoes acid-catalyzed cross-linking making it highly modified in the form of acid-insoluble lignin or Klason lignin. It should be noted that a small portion of the polysaccharides undergoes breakdown to furanic compounds and hydroxymethyl furan.

Subsequently, the reaction mixture is filtered using a porcelain, medium porosity ceramic filter crucible. The residue in the crucible primarily contains acid-insoluble lignin components but for certain biomass sources, it also contains some protein that must be accounted for in the residue. The acid-insoluble Klason lignin is determined by first drying the crucible at 105 °C and measuring the weight of the dried sample as well as the sample after ashing 575 °C. Residual ash (but not necessarily equivalent to total ash) is accounted for and removed from the calculation of the acid-insoluble lignin. For high protein content samples, residual protein is accounted for via nitrogen elemental analysis of the acid-insoluble residue, where the nitrogen percentage is converted into

protein content by a generic multiplier of 6.25 although, a more accurate multiplier between 5.1 and 6 has been determined for a number of species [61, 62]. ASL is analyzed in the filtrate using UV–vis spectroscopy be relating the absorbance at $\lambda = 240–320$ nm to the total concentration, through the absorptivity coefficient (maintaining a given path length). Note that this analysis is based on the Beer–Lambert Law and is a highly accurate and simple method to determine the concentration. Careful selection of the absorbance range (usually below 1) and absorptivity coefficient is required based on the biomass type and the pretreatment method.

4.8.1 Analyzing Filtrate by HPLC for Monosaccharide Contents

Many of the monosaccharides are epimers of each other; hence they have the exact same molecular formula, similar ring structures but differ in conformations of the hydroxyl and hydrogen groups attached to the different carbons on the ring. This similarity makes it difficult to determine the exact amount of components without separating them in some manner. A common method of separation is liquid chromatography that partitions components between two phases, typically a mobile fluid phase and a solid stationary phase. Chromatography was first developed by M. Twsett to separate chlorophyll pigments, as their separation on a $CaCO_3$ column left bands of color (chroma is color in Greek). Nowadays high-performance liquid chromatography equipment couples a column system to an online detection system to determine the concentration. These detection systems can be simple for light absorbing compounds, such as UV–vis detectors, to detectors that measure the change in refractive index (RI) of the solution as a function of concentration, or a pulsed amperometric detector that measures the change of electrical current. The latter has gained in popularity for systems for dedicated sugar analysis as it is very sensitive for detection of sugars at very low concentrations.

4.8.2 Choosing the HPLC Column and Its Operating Conditions

Figure 4.2 shows the chromatogram of a mixture of cellobiose, glucose, xylose, and arabinose using Bio-Rad® Aminex 87**H** column and detected with an RI detector. This column can separate cellobiose, glucose, xylose, and arabinose. The column is not suitable for the analysis of lignocellulose with high mannose content, such as softwoods because mannose is co-eluted with glucose. The advantage of this column is that it is robust and will not be greatly impacted by fluctuations of the pH of the eluent. It is commonly used to analyze glucan digestibility of biomass, as glucose is released based on the specificity of the cellulase hydrolyzing cellulose. Figure 4.2 shows an example of the monosaccharide elution profile using RI detector.

To analyze samples with high mannose content, the Bio-Rad® Aminex 87**P** column is effective to separate out all the hydrolyzed monosaccharides (glucose, xylose, galactose, arabinose, and mannose); however, rigorous protocols must be used to limit pH fluctuations that will impact the life of the column.

Other components of biomass can make up a significant mass portion. In hardwoods, the hemicelluloses are highly acetylated and they can make up to 10% of the mass of the isolated xylan corresponding to 2–5% of the wood. Additionally, uronic acid branches of hemicelluloses can compose upwards of 2–6% of the wood [63]. Acetyl groups can be readily determined by measuring the acetic acid concentration in the hydrolysis liquor via HPLC (high-performance liquid chromatography) with an RI detector. The

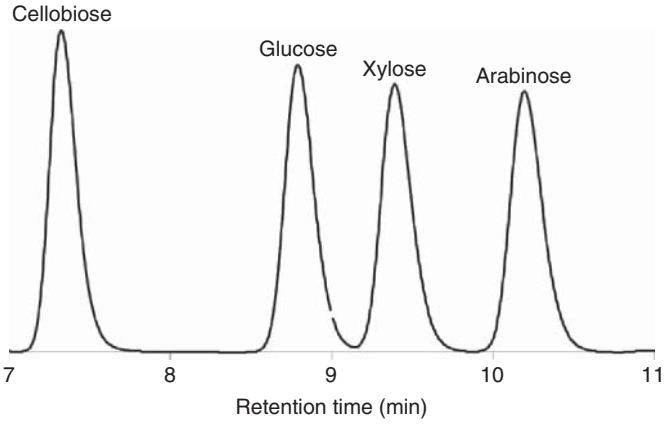

Figure 4.2 HPLC chromatogram of four monosaccharide standards separated by Bio-Rad® Aminex 87P column at 60 °C, flow rate of 06 ml min^{-1} of 4 mM H_2SO_4.

uronic acid side groups such glucuronic acid or galacturonic acid can be detected with HPLC but typically specific protocols, different from the main chain polysaccharides, must be established as their interactions with the column change their retention time significantly. While HPLC methods are common to quantify sugar components, gas chromatography (GC) methods were also developed for sugar determination. GC methods require the reduction of the monosaccharides into their nonreducing alditol form and derivatizing into acetates with acetic anhydride. The samples need to be isolated from the derivatizing solution because unreacted compounds impact peak resolution. While the method involves additional steps that would make screening 100s of samples more difficult relative to direct injection with HPLC, it is an accurate alternative for carbohydrate analysis (Table 4.2).

4.9 Determining Cell Wall Structures Through Spectroscopy and Scattering

4.9.1 Probing the Chemical Structure of Biomass

The structure of carbohydrate contributes to the fiber properties and ultimately affects the product quality. Many techniques, such as X-ray diffraction (XRD), cross-polarization/magic angle spinning (CP/MAS) ^{13}C NMR [15–17, 66, 67], Fourier-transform infrared spectroscopy (FTIR), and Raman spectroscopy [68–70] have been employed to determine chemical structure and local environment of the polysaccharides. These techniques are nondestructive and can be used with biomass in the as-received state. The degree of crystallinity is one of the commonly used parameters to probe cellulose characteristics of biomass. Herein, we discuss the resulting information from these techniques and how to correlate the obtained information with the chemical structure of biomass.

Table 4.2 Advantages and disadvantages of biomass characterization methods and techniques.

Techniques	Advantages	Disadvantages
Two-step acid hydrolysis	• Quantitative • Well established and well accepted	• Destructive • Analysis time by HPLC can be long • Labor intensive • Toxicity from acids and corrosion products
CP/MAS ^{13}C NMR	• Detailed analysis • Nondestructive • Selective	• Low throughput • Insensitive • Long analysis time • Expensive • Automation is challenging
XRD	• Fast analysis • Nondestructive • Results are qualitative and quantitative	• Low throughput • Peak convolution • Safety due to X-ray
FTIR	• High-throughput capabilities • Nondestructive • Fast analysis	• Qualitative • Peak convolution • Very sensitive to moisture • May require specific sample preparation (e.g., KBr)
Raman spectroscopy	• Not sensitive to moisture • Easy sample preparation • Multiple excitation sources including ultraviolet (UV), near-infrared (NIR), and visible (VIS), so this can tailor for various analytes • High throughput • Applicable to solid, liquid, and gas	• Weak signal • Sensitive to strayed light
Pyro-GC/MS	• Only small amounts of samples are needed • Easy sample preparation • No need to isolate lignin • Can be high throughput	• Destructive • Complex data analysis
Solution-state NMR	• Detailed structural information • Quantitation can be done without calibration standards	• Destructive • Semiquantitative • Analysis can be long • Insensitive • Expensive • Automation is challenging • Complex set-up due to inter-relationships between sample concentration, sample solubility limit, and acquisition time
GPC	• Fast analysis • A wide array of available detectors for the analysis of various polymers including multi-angled light scattering (MALS), ultraviolet (UV), and refractive index (RI)	• A number of calibration standards are needed for accuracy • Destructive • Semiquantitative • Complex analysis for polydispersed polymers

Source: Adapted from Refs [64, 65].

4.9.1.1 X-Ray Diffraction (XRD)

XRD is commonly used to analyze the degree of crystallinity of cellulose. As mentioned earlier, cellulose is always deposited as bundles or aggregates of cellulose chains. The chains have symmetry and as a result diffract X-rays according to the structure of the unit cell. Interference peaks of the diffracting electromagnetic radiation arise from the specific spacing of subatomic particles arranged in the molecular structure. In powder diffraction, there is a randomization of the scattering plans forming a concentric pattern with the angular intensity (2θ) directly related to the spacing (Å) of diffracting planes through Bragg's Law. The original indices for the diffraction of cellulose peaks have been revised for the unit cell, the most basic repeating pattern of the crystal, and it is generally accepted to report the diffraction peaks with Miller indices for cellulose I_α as (100, 010, and 110) and cellulose I_β as ($1\bar{1}0$, 110, and 200).

As highly ordered arrangements of polymers dramatically differ in mechanical properties as well as access to internal surfaces, the crystallinity of cellulose is seen as a key factor governing wood properties, fiber quality, as well as bioconversion. The degree of crystallinity can be expressed by CrI. The index, as the name implies, is not an absolute number but a comparative method to determine the relative portion of symmetry within the biomass. Sample preparation is quite easy for analysis, however, drying history has a large impact on the results, and sample preparation should be considered carefully and reported in the analysis. Because of the low bulk density of cellulose fibers, typically samples are pressed into a pellet to increase the sample per unit volume. Artifacts can sometimes occur as distortion in certain planes can occur causing orientation as samples are compressed. Samples of small amounts can be placed on quartz substrate for analysis and the sample substrate can be subtracted as background from the diffractogram. There are multiple ways to calculate the CrI from the biomass as listed. The three methods of calculating CrI are portrayed in Figure 4.3 [15]: Segal method [71]; peak deconvolution [15]; and amorphous subtraction [72]. The Segal method is the most common method for calculating CrI using the relationship between (002) and the amorphous region as follows:

$$\mathrm{CrI} = \frac{I_{(002)} - I_{(am)}}{I_{(002)}} \times 100$$

where $I_{(002)}$ is the height of the (002) and $I_{(am)}$ is the height of the amorphous region.

The peak deconvolution method uses the idea that five crystalline planes of cellulose I_α, corresponding to (101), ($10\bar{1}$), (021), (002), and (404) are scattered on the amorphous region (Figure 4.3b). So these crystalline and amorphous planes can be deconvoluted, and the CrI value can be determined from the ratio of the crystalline area over the total area [15]. The peak deconvolution/fitting peak fitting is subjective to the user and cannot always be repeated with accuracy. Hence, the peak deconvolution has to be done with caution. The amorphous subtraction method is done by subtracting the spectrum of interest with the amorphous standard [72], which can be hemicellulose, lignin, or phosphoric acid swollen cellulose (PASC). The CrI can be calculated from the ratio of the crystalline area over the total area after all peaks are deconvoluted. Out of the three methods, the Segal method appears to provide the highest value of crystallinity.

It should be noted that most of the analysis is related to the characteristics of cellulose either in the form of the cell wall, the pulp fiber, or micro-/nanocellulose. However, hemicelluloses are amorphous in the cell wall can be crystallized through

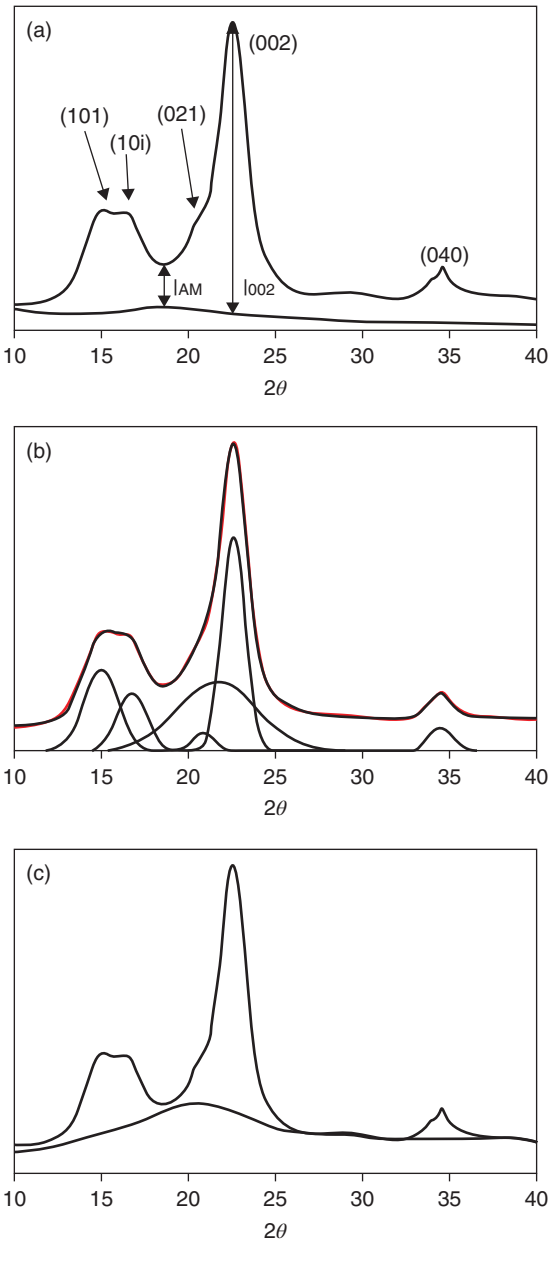

Figure 4.3 X-ray diffraction spectra of microcrystalline cellulose (Avicel PH-101) shows three methods for calculating CrI: (a) Segal method; (b) peak deconvolution method; and (c) amorphous subtraction method.

debranching and careful precipitation. Hemicelluloses can crystallize as hydrates and the diffractogram will change depending upon the amount of moisture present. Other studies have analyzed technical lignins for periodicity in their structure.

4.9.1.2 Cross-polarization/Magic Angle Spinning (CP/MAS) ^{13}C NMR

CP/MAS ^{13}C NMR or also often known as solid-state nuclear magnetic resonance (ssNMR) can be used to observe changes of inter- and intramolecular hydrogen

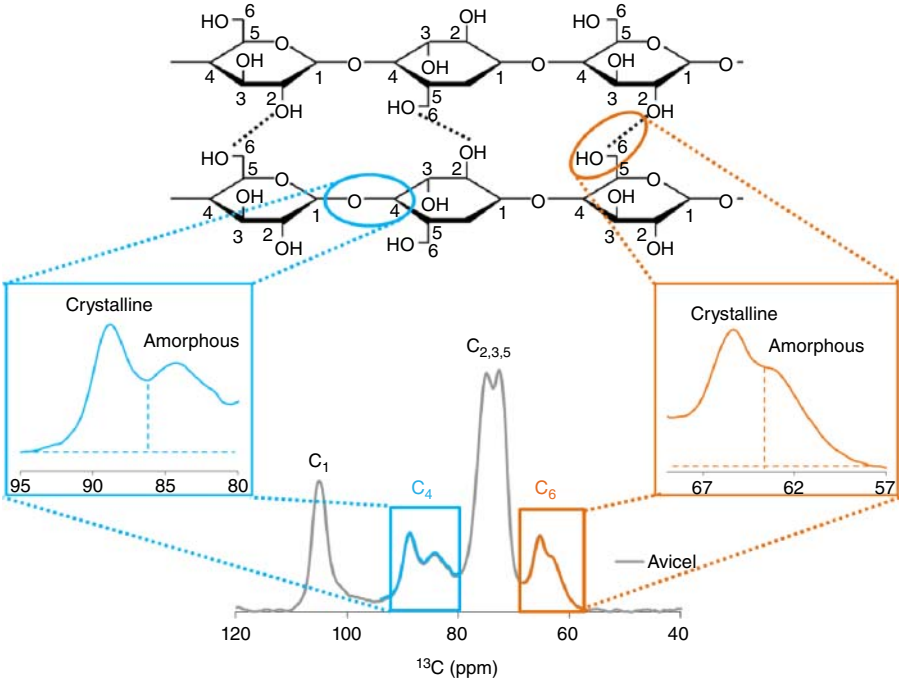

Figure 4.4 Illustration of information obtained from CP/MAS ^{13}C NMR spectrum of microcrystalline cellulose. C_4 and C_6 regions are typically used for CrI determination and evaluation of changes in inter-/intramolecular hydrogen bonding.

bonding of polysaccharide chains [15, 16, 73]. This method uses radio electromagnetic radiation to perturb spins of isotopes (with an odd number of spins) and the localized environment relaxes the perturbed spins back to its normal state. For cellulose, each carbon has a response to this perturbation. Figure 4.4 shows the spectrum of microcrystalline cellulose (Avicel). The C_1, C_4, and C_6 carbons are differentiated in the spectrum, while there is considerable overlap in the $C_{2,3,5}$ signals. C_4 region is commonly used to determine CrI [67], and C_6 region is used to observe changes in hydrogen bonding among cellulose chains. CrI can be determined by two methods: (i) C_4 peak deconvolution and (ii) amorphous subtraction.

For polymers in a highly organized state, localized interactions among cellulose chains will cause their response to differ. The core chains of cellulose microfibrils will be in a distinct local environment relative to the chains on the surface of the microfibrils. Hence, the relative amount of crystallinity in the sample can be determined using the C_4 peak deconvolution (i.e., $X/(X+Y)$ in Figure 4.4).

Similar to XRD, C_4 peak deconvolution of the NMR spectrum is subjective, and the results are user dependent to a degree. However, the method is widely used to report the relative crystallinity of cellulose as the signal intensities are directly related to the amount of species present. Caution should be taken because hemicellulose components also generate signals in the region that corresponds to the amorphous cellulose signals. To avoid falsely assigning signals to amorphous cellulose, the signal can be further deconvoluted for the individual contributions of the signal to the hemicellulose,

amorphous cellulose, and crystalline cellulose [74]. Furthermore, the moisture content of the sample can cause slight increases in CrI by 5% [6]. Finally, it is interesting to note that the signal intensity of the deconvoluted peaks has been used to estimate the microfibril size of hydrolyzed samples, with all hemicelluloses removed, fitting the fractional intensity of surface chains to a rectangular cross-sectional model [74].

The amorphous subtraction method is done the same way as that by XRD. The CP/MAS ^{13}C NMR spectrum of interest is subtracted by the spectrum of the amorphous component of lignocellulose (i.e., hemicellulose, lignin, and PASC). Then, the area ratio is used to determine CrI.

4.9.1.3 Fourier-Transform Infrared Spectroscopy (FTIR)

FTIR is one of high-throughput analyses that can provide both qualitative and quantitative information about the chemical characteristics of biomass and the isolated components. FTIR works on the principle of a harmonic oscillator where the vibrational energy of bonds corresponds with the energy of certain frequencies of infrared light [75]. Hence bond strength and the mass of elements bonded together (and how the localized environment influences them) have corresponding bond energy that matches the energy of certain frequencies of infrared light. This mechanism causes certain frequencies of light to be absorbed by the corresponding bond type if the dipole moment is changed as a function of bond distance during excitement. The resulting spectrum of the Fourier-transform signal reveals aspects of the chemistry of the material. Infrared spectroscopy is typically divided into two categories based on the wavelength of the radiations used: near-infrared spectroscopy (NIR) has been developed to be used in field or industrial quality control environments, while mid-infrared (MIR) spectroscopy is typically found in most research laboratories for chemical analysis.

FTIR spectroscopic analysis of biomass requires some manipulation of the resulting spectrum. Because CO_2 and moisture can absorb electromagnetic radiation, there is always a background spectrum that needs to be subtracted from the sample spectrum. Usually, the background spectrum is acquired just prior to the analysis of a sample, and the software is designed to automatically subtract the background. Often though there is a distorted baseline because of scattering from the sample and the baseline should be adjusted by moving the spectrum to zero for regions where there is no absorbance. This shift can be automatically adjusted or user defined, but should be done with attentiveness to ensure a uniform procedure between samples. After the baseline is corrected, samples are often normalized so the intensity of absorbance is plotted in a way to see comparative changes in the spectra among samples.

Both NIR and mid-FTIR methods have been used to understand cellulose structure. For example, mid-FTIR has been correlated to the CrI [76]. The ratio of select signals that arise because of order can be correlated to the CrI determined from using other methods like XRD. Changes in cellulose crystallinity in the 850–1500 cm^{-1} range were observed by Nelson and O'Conner [69, 70]. The total crystallinity index (TCI) and lateral order index (LOI) were proposed from the ratio of 1420/893 and 1375/2900 cm^{-1}, respectively.

The molecular orientation of cellulose during the formation of wood cell wall can be analyzed by observing changes of bands at 898 (ν_{as}(ring), anomeric vibration at β-glycosidic linkage) and 1160 (ν_{as}(COC), COC antisymmetric stretching) [77]. Both bands are present in FTIR spectra of microcrystalline cellulose and PASC [17], suggesting that FTIR is not an absolute technique [15]. Additionally, the transformation

of cellulose into cellulose II during the mercerization process, exposing cellulose fibers to aqueous alkali, causes significant peak changes in the corresponding spectra [78]. This point highlights the sensitivity of FTIR analysis to detect supramolecular changes without significant changes to the chemistry of the polysaccharide [79].

Furthermore, FTIR is widely used to confirm the derivatization of polysaccharides. During esterification, two significant spectrum changes occur that are readily notable. The prominent hydroxyl stretching is decreased while absorption in the carbonyl region is increased. These data are qualitative and can show the successful modification, but it typically lacks the quantification of substitution level. However, like CrI, a calibration curve can be created where the area of the absorbance region is plotted as a function of the degree of substitution [80]. This technique especially works well for cellulosic esters because there is not significant absorption from other functional groups in this range of 1860–1690 cm^{-1}, allowing for the quantification of the signal according to Beer–Lambert Law. Interestingly, the technique allows for the analysis of small quantities of esters compared to the other methods such as titration and ^{1}H NMR [80].

As the mechanism of IR analysis is the harmonic oscillator model where IR radiation is absorbed and converted into energy of molecular rotation [75], the molecular vibrations have harmonics at higher wavenumbers (higher frequency) in the near-field IR from 10,000 to 4000 cm^{-1}. For NIR analysis, a fiber-optic probe both delivers the IR radiation and detects it. Sampling is straightforward as reflected light from the material is detected accounting for the light that is absorbed and also scattered. Once a given set of calibration standards is made, NIR is powerful in detecting specific changes of materials. It has been used to analyze the moisture content of biomass for biofuels [81] to follow cellulose structure changes during alkali treatment [82]. With multivariate component analysis, the chemical composition of biomass can be correlated with the NIR spectra for all the major polysaccharide components, lignin, and even extractives [83].

4.9.1.4 Raman Analysis

Raman spectroscopy is another form of vibrational spectroscopy analysis. Raman signals are generated from inelastically scattered light, where bonds are excited to an elevated state of the monochromatic radiation, and light energy released from the molecule returns the bond to a lower energy level. Because energy is quantized it is analogous to a person who boarded an elevator on the second floor (an excited state) and rode the elevator to the top floor, and decided to return the first floor (a different energy state). The energy lost, inelastic scattering of light from starting and ending at two different levels, is related to the type of bond. Like FTIR, the Raman spectrum consists of signal intensity as a function of wavenumber, which is the difference in energy from the impinging light and the energy loss between starting and ending at two different energy levels. Complimentary to FTIR, where the signal is generated because of a change in dipole moment of the molecule with respect to the distance of atoms, Raman signals are generated from the polarizability of the molecule or the relative ease that an electron cloud can be disturbed. This mechanism means that carbon–hydrogen signals are much stronger than hydrogen–oxygen signals, making water relatively transparent for this method of analysis. Like FTIR, the local molecular environment greatly impacts the signals and this method can be used to examine different crystalline structures of cellulose [84].

The drawback to this analytical method is that fluorescence can saturate the signal blocking the measurement of the bonds of interest. Auto-fluorescence can be

problematic with lignin-containing compounds. However, this issue can be mitigated to a point depending upon the excitation laser in the spectroscope. Longer wavelength lasers in the 700 nm region can avoid some of the issues faced with this measurement technique. The drawback of using a longer wavelength is a loss of signal intensity, so the power of laser and detectors need to be adjusted accordingly.

The method has received much attention to do two- and three-dimensional (3D) label-free mapping of chemical functional groups [85]. Hence, the spatial resolution of functional groups can be determined if the spectroscope is coupled to a confocal laser microscope. While not quantitative in nature, the method allows the determination of the relative distribution of components within the biomass cell wall of microtomed samples. Typically the spatial resolution is one micron, and this allows changes in the cell wall to be determined from the cell wall corners and middle lamellae to the innermost portion of the S3 layer [86]. However, Raman analysis has also been coupled to atomic force microscopy analysis providing detailed surface and chemical resolution [84].

4.10 Examining the Size of the Biopolymers: Molecular Weight Analysis

The molecular weight of polymers is a key component in understanding mechanical properties and processibility of materials in the solution and melt state. For the strength of polymeric materials, one can imagine long thread-like molecules entangling together, and the greater the length of the molecules the more entanglements. Because polymer chain size is not uniform, an average of chain sizes is used to describe the molecular weight. For polymer characterization typically the first moment or the second moment of the distribution is used to describe the materials. The first moment is referred to as the number-average molecular weight (M_n) and is the ratio of the sums of the total number of molecules with a specific size of the polymer to the sum of the total number of polymers (providing a mean related to the summation of the mole fraction). The second moment is referred to as the weight average molecular weight (M_w) and is found by the summation of the number of molecules multiplied by the square of the molecular weight of each fraction divided by the summation of the molecular weights (summation of the number of molecules times the size of each chain). As the molecular sizes are a distribution, the ratio of the M_w over the M_n provides insight into the breadth of the distribution. This ratio is normally called the polydispersity index (PDI) [87]. M_n, M_w, and PDI can be expressed as

$$M_n = \frac{\sum N_i M_i}{\sum N_i}$$

$$M_n = \frac{\sum N_i M_i^2}{\sum N_i M_i}$$

$$\text{PDI} = \frac{M_w}{M_n}$$

The index number, i, represents the number of different molecular weights in the polymer sample and N_i is the total number of moles with the molar mass of M_i.

Gel permeation chromatography (GPC) is used to quantify the molecular weight distribution of polymers. With this technique, polymers are separated based on their hydrodynamic radius by forcing the polymer solution through a column containing particles of varied size with micropores. Large polymer chains are eluted in the column in short times because their hydrodynamic size is larger than the micropores on the bead surface in the column. As the chains elute, the concentration in the solution is determined via UV and or RI detectors. A profile of chain sizes is developed as a function time, known as the molecular weight distribution. This profile holds the key information about one of the most fundamental pieces of information about polymers that impacts polymer performance in the liquid and solid state. The problem for biopolymers like lignin is that SEC (size-exclusion chromatography) is not based on an absolute measurement, only the time it takes for the polymer chains to slip through the column. Calibrated standards can be used to get around this issue by passing materials like polystyrene or pullulan with defined molecular weights through the system because of the product of the intrinsic viscosity and molecular weight are not unique and can be directly related to each other. This method works well for many types of samples and is referred to as the "universal calibration method" [88]. For absolute measurements, other detectors can be connected to the system such as a multi-angle light scattering detector (MALS). The detection system provides an absolute molar mass and the root mean square (rms) radius of the polymer based on light scattering principles that relate the angular dependence of the scattered light to the polymer chain size and structure. MALS can be used to determine the M_w as the turbidity/scattering intensity is related to the reciprocal of the number-average molecular weight when the scattering (and concentration) is extrapolated to zero. The drawback of MALS is that fluorescence emitted from the sample can negatively impact the characterization of the sample. This issue is critical in lignin molecular weight analysis, and caution should be taken for samples that are contaminated with lignin (unbleached xylan). However, instrumentation that includes longer light wavelengths, and filters can be used to partially circumvent this issue.

The difficulty of dissolving cellulose makes molecular weight determinations problematic. In an ideal system for cellulose characterization, the GPC system utilizes a cellulose solvent, such as DMAc with 0.1 M LiCl. Several errors can occur through the dissolution process of cellulose, and molecular weights should be carefully calculated based on adjusting the mass of DMAc associated with cellulose [89]. Problems have occurred also because of the limited solubility of some high-molecular-weight celluloses. The other option to characterize the molecular weight of cellulose is based on making a cellulose derivative that is soluble in more common solvents. Tricarbanilated cellulose, where the hydroxyls are replaced by phenyl groups through a urethane linkage is one method where derivatization has limited chain degradation [90]. The derivatizing agent, phenyl isocyanate, is highly reactive and must be handled with extreme caution.

Other molecular weight determination methods involve chain end analysis or viscosity measurements that provide insight into the size but not the size distribution. The former provides information about the number-average molecular weight because it is determined from the number moles of end groups to the total number of repeat units. For polysaccharides, each chain is capped by a reducing end of the polysaccharide, which can be used to determine the number-average molecular weight [91]. The ratio of the number of reducing ends can be found through titration, which is simple; however,

for cellulose in fibrous form, there must be a solubilization step that first occurs [92]. Other more soluble polysaccharides can be analyzed directly using solution-state NMR to determine the number-average degree of polymerization (DP) [93]. HPLC can also be used if the chain end has a specific saccharide termination step. For glucuronoxylans, there is a rhamnan unit associated with each end unit [94–96]. The ratio of the number of xylose units to the rhamnose units provides a simple method for molecular weight determination of xylan. The drawback to this method is that pectin-based material from the compound middle lamella may influence the results.

Using dilute viscosity measurements, the viscosity average molecular weight M_v can be determined through the relationship of the Mark–Houwink–Sakurada equation. This molecular weight falls between the first and second moment of the distribution. The viscosity of a solution relates how chains interact with each other. On a relative basis, related to the resistance to flow, the viscosity of the solution can be easily calibrated to a technique for a simpler test, named the falling ball method. Cellulose pulps are dissolved in cupriethylenediamine at 1% solution, and the measurement is based on the time it takes for an aluminum ball to drop through the solution [97]. The method is developed for quality control analysis.

Like cellulose, lignin is often derivatized in order to solubilize in common solvents like tetrahydrofuran [98]. However, polar organic solvent, such as dimethylsulfoxide (DMSO), dimethylformamide (DMF), and DMAc [99] have been used to characterize lignin without derivatization. A hybrid method has used ion-pair chromatography for lignin analysis, modifying lignin simply through adsorption, where lignin has a strong association with cationic amines [100]. Additionally, aqueous systems have been applied to hydrophilic lignin samples dissolved in an aqueous alkali. The choice of solvents, pH, and ionic strength influence the elution profile of lignin. It should be noted that polymer solutions require each polymer chain to be solvated. This idea seems straight forward, for example, with an experiment where cellulose triacetate is immersed in acetone; the sample disappears into the solution as the individual chains lose contact with each other. However, for dissolving a technical lignin-like a hardwood kraft lignin, the sample disappears into the solution, yet it is not fully dissolved. Lignin has a high degree of intermolecular associations based on its aromatic structure, and there is a significant time component to dissolution. Many treatment methods have been published on the subject, and careful attention to reporting these details should be given. This issue arises because lignin and lignin derivative solutions can be aged, and the molecular weight profiles show differences and is dependent upon the time of solution preparation and the temperature at which the material is stored. This change is also seen in the RI increment, as dn/dc values can take several days to stabilize [101]. Different additives can be introduced to solutions to limit these aggregations such as iodine [102]. To dissolve lignin in a common solvent like THF, acetylation procedures are used by reacting lignin with acetic anhydride over pyridine [103].

4.11 Intricacies of Understanding Lignin Structure

Because lignin is an amorphous biopolymer created by the oxidative coupling of monolignol(s) (i.e., *p*-coumaryl alcohol, coniferyl alcohol, and/or sinapyl alcohol), there are a number of interunit linkages that provide some level of complexity to

the structure. Additionally, the structure changes dramatically during isolation and processing. Utilization and exploitation of this biopolymer hinges on understanding its structure and connecting it to its performance and some specific methods are outlined in the following sections.

4.11.1 ^{13}C NMR

As mentioned earlier, NMR relies on the detection of odd-numbered isotopes such as ^{13}C, and these signals can be quantitative from the population of atoms in the material. As such, ^{13}C NMR can be performed to examine the entire structure of soluble lignins to determine the presence of interunit linkages (e.g., β-aryl ether linkages), condensed and uncondensed aromatic and aliphatic carbons, H/G/S ratio, and the total amount of functional groups. The advantage of this technique is that one is able to study the entire soluble lignin structure intact without acetylation. The downside is that these ^{13}C nuclei are not naturally abundant, so high lignin concentration and/or long acquisition time are required. In some cases, a relaxation agent, such as chromium (III) acetylacetonate, can be added to the lignin solution to help provide a complete relaxation of nuclei. This additive reduces the time it takes for the atoms to go back to their unperturbed state (T_1), allowing better signal-to-noise ratio at shorter collection times. After collecting the data, the spectrum reveals all the different carbons in a sample (such as carbons involved in the aromatic structure, carbons in a carbonyl bond, or aliphatic carbons). The area for each of these peaks can be integrated and the ratio of peaks can be used to characterize the sample. When normalizing for the number of carbons in the signal, the ratio of peak intensities can be used to determine the functional group or interunit linkage per C_6 or C_9 [104]. The technique is sensitive to distinguishing different carbonyls attached to the lignin such as carboxylic acids and aldehydes, which are related to decomposition mechanisms. Figure 4.5 shows the ^{13}C NMR spectra of milled wood lignin (MWL) [44] isolated from loblolly pine by Bjorkman method [105]. The inset reveals the aliphatic region of the MWL and acetylated MWL (MWL-Ac). The ^{13}C NMR spectrum can be divided into regions shown in Table 4.3.

The integration of the aromatic region ($I_{160–103}$) can be set to a value of 6.12, representing all aromatic carbons plus a contribution of 0.12 per 100 aromatic units from the side-chain carbons of coniferyl alcohol and coniferaldehydes. Then integration of all moieties (e.g., methoxyl content) will be based on the aromatic ring. For example, after setting the $I_{160–103}$ to a value of 6.12 and integrating the 57–54 ppm range, the methoxyl content can be expressed as 0.95 methoxyl group per aromatic ring.

4.11.2 ^{31}P NMR

A critical aspect in lignin chemistry when synthesizing new compounds is the absolute number of functional groups per gram of isolated lignin. This information is required so the proper stoichiometric ratios are used when converting lignin into copolymers or soluble derivatives. Hydroxyl functional groups of lignins can be identified by a ^{31}P NMR technique, involving the phosphorylation of lignin with 2-chloro-4,4,5,5-tetramethyl-1,3,2-dioxaphospholane (TMDP) [106]. The reaction of TMDP with lignin hydroxyl functional groups is illustrated in Figure 4.6a. TMDP reacts with hydroxyl functional groups to give phosphite products, which are resolved by ^{31}P NMR into various regions from aliphatic hydroxyl, phenolic, and carboxylic acids

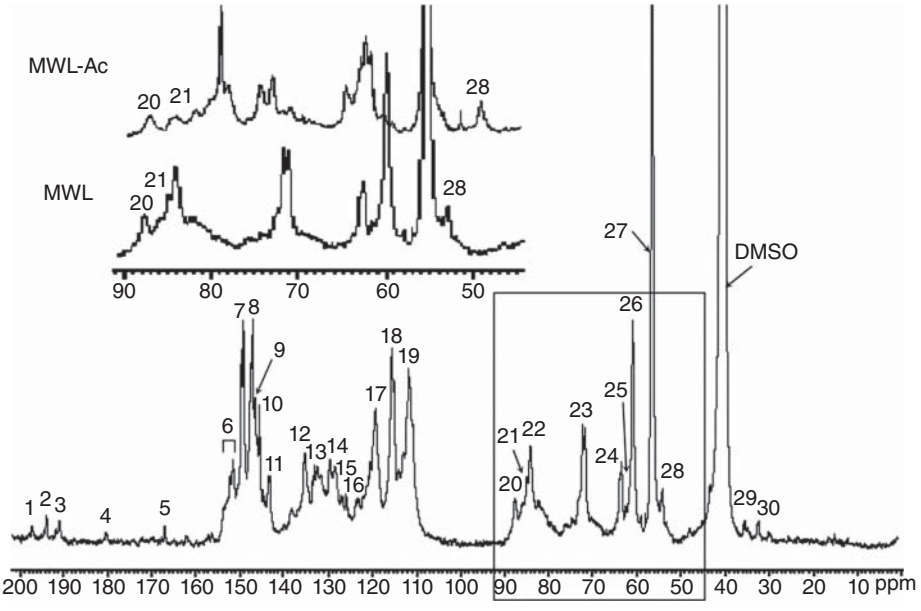

Figure 4.5 ^{13}C NMR spectrum of MWL isolated from pine shows various spectral regions.

Table 4.3 ^{13}C NMR chemical shift ranges and integration regions of all moieties.

Spectral region	Chemical shift range (ppm)
Methoxyl content	57–54
Aromatic methane carbons	125–103
Aromatic carbon–carbon structures	141–125
Oxygenated aromatic carbons	160–141
Carbon from carbonyl-type structures	195–190
Carbon from carboxyl-type structures	176–163
Degree of condensation (calculated by 3.00-$I_{125-103}$)[a)]	125–103
Aliphatic hydroxyl content	171–168.5
Phenolic hydroxyl content	168.5–166

a) $I_{125-103}$ represents the integration from 125 to 103 ppm.
Source: Adapted from Ref. [44].

groups as illustrated in Figure 4.6c. The reaction occurs quickly, and the samples must be analyzed in short time periods after the reaction period because of the formation of HCl as a by-product. Peak integration of the spectrum relative to an internal standard, endo-*N*-hydroxy-5-norbornene-2,3-dicarboximide (e-HNDI) or cyclohexanol, allows the quantification of the moles of functional group per gram of sample. Different phenolic groups can be distinguished depending on their origination from different monolignols, such as sinipyl alcohol versus coniferyl alcohol, which is also helpful in

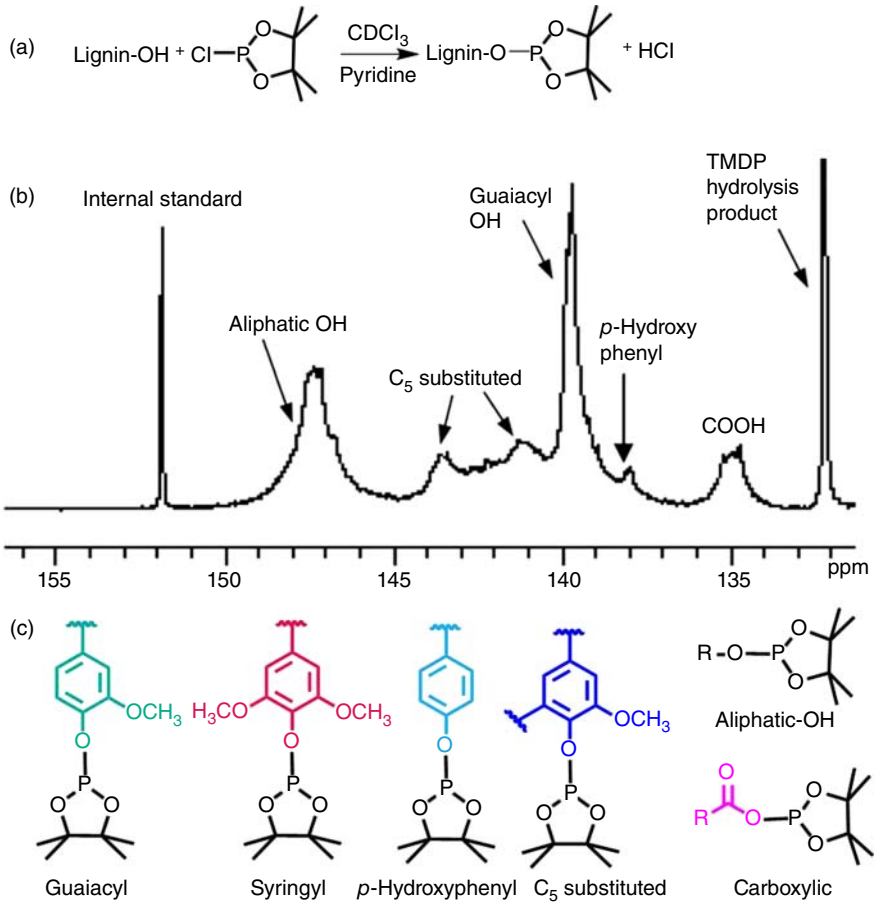

Figure 4.6 Phosphorylation of lignin with 2-chloro-4,4,5,5-tetramethyl-1,3,2-dioxaphospholane (TMDP) is fast and reaction products (c) are shown in ^{31}P NMR spectrum (b) and lignin modified (a).

examining the breakdown products. Figure 4.6b shows an example of the ^{31}P NMR spectrum of a softwood lignin derivatized with TMDP using HNDI as internal standard [107]. Typical chemical shift ranges and spectral regions for integration are shown in Table 4.4.

4.11.3 2D HSQC

2D ^{1}H–^{13}C solution-state NMR spectroscopy has been developed to reveal detailed information about lignin structure. This technique offers a semiquantitative analysis of lignin structure of ball-milled lignocellulose without extraction and acetylation of lignin. Dimethyl sulfoxide-d_6 is commonly used as a lock solvent during the procedure. In some cases, a minute amount of co-solvent, such as 1-methylimidazole (or *N*-methylimidazole) [48], pyridine [4, 45], and 1-ethyl-3-methyl-imidazolium acetate [27, 46], can be added to aid lignocellulose solubility, increasing solution viscosity and in turn decreasing the relaxation time. Figure 4.7a, b, and c shows the 2D HSQC

Table 4.4 ^{31}P NMR chemical shift ranges and integration regions of hydroxyl moieties.

Spectral region	Chemical shift range (ppm)
Aliphatic	145.4–150.0
Phenols	137.6–144.0
C_5 substituted	140.0–144.5
β-5	~143.5
Syringyl	~142.7
4-*O*-5	~142.3
5-5	~141.2
Guaiacyl	139.0–140.2
Catechol	~138.9
p-Hydroxyphenyl	~137.8
Carboxylic acid	133.6–136.0

Source: Adapted from Ref. [107].

(heteronuclear single-quantum correlation) spectra of enzymatic mild acidolysis lignin (EMAL) isolated from hardwood [108]. These spectra show the C–H coupling in aliphatic, aromatic, and anomeric regions. Aliphatic region reveals lignin interunit linkages. Important correlations include methoxyl groups, β-aryl ether (β-O-4), phenylcoumaran (β-5), resinol (β-β), and dibenzodioxocin (5-5/4-O-β). Aromatic region reveals the difference in the H:G:S distributions in the lignins. Anomeric region shows polysaccharide anomerics; however, overlapping of peaks makes it hard for interpretation. For EMAL, most carbohydrates were hydrolyzed by enzymes and acid. Hence, only a trace amount of carbohydrates were observed. Figure 4.7d shows the anomeric region of switchgrass, consisting of cellulose and hemicelluloses.

HSQC analysis is semiquantitative, and it can be used for both structural identification and estimation of the relative abundance of interunit linkages, H:G:S ratios of lignin, profiling cellulose and hemicellulose [4, 109, 110]. The relative abundance of each respective interunit linkage is then calculated as the percentage of integrals of total linkages. For determining H:G:S ratios of lignin from integrating cross-peaks from HSQC spectra, it should be noted that the G_5 cross-peak is not suitable to use for quantification of the G content because G_5 cross-peak overlaps with the $pCA_{3,5}$ and $H_{3,5}$ correlations. G_6 is *para* to the methoxy group, increasing the chance to participate in condensation reactions. Hence, G_2 cross-peak is typically used for quantification of the H:G:S ratio [111, 112].

The C_2 and C_6 positions of syringyl units in lignin rarely get substituted [113]. Hence, the overall C_9 units in lignin can be estimated by

$$C_9 \text{ units} = \frac{1}{2} S_{2,6} + G_2$$

The C_9 unit value can be used to normalize the interunit linkages of lignin, which can be expressed as percent of C_9 units. For example, β-O-4 content is 49.1% of C_9 units.

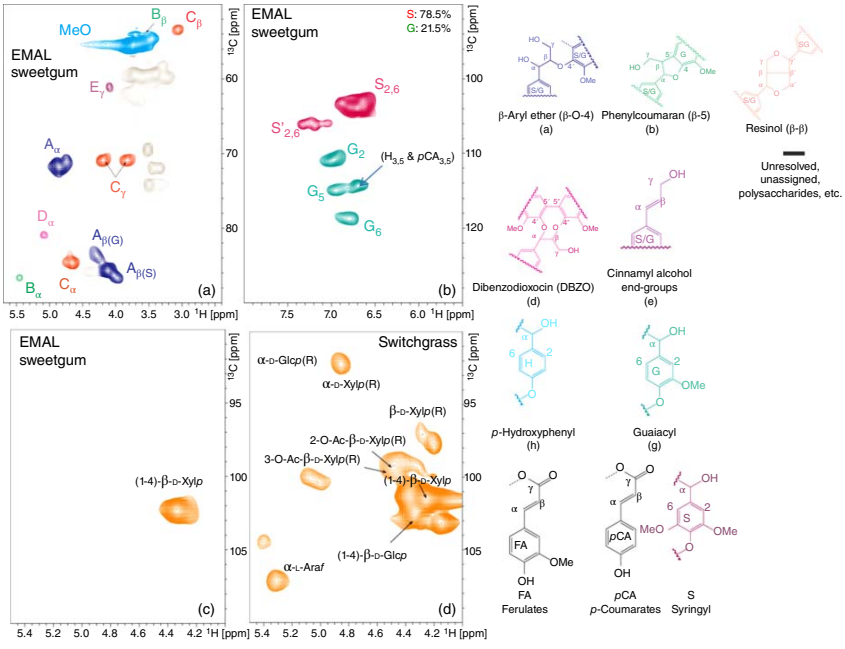

Figure 4.7 The 2D HSQC spectra of enzymatic mild acidolysis lignin (EMAL) isolated from hardwood [108].

It should be noted that all of the integration of cross-peaks should be done at the same contour level.

Table 4.5 summarizes important chemical shifts and assignments of cross-peaks of interunit linkages and/or subunits in HSQC spectra of lignin.

The 2D HSQC has proven to be a powerful tool to evaluate changes in transgenic plants [28, 29, 115, 116] and changes due to chemical and biological modifications of plant biomass [46, 47, 52, 117–123].

Table 4.5 Assignments of carbohydrates/lignin ^{13}C–^{1}H correlation peaks in the 2D HSQC.

Region	Label	δ_C/δ_H (ppm)	Assignment
Aliphatic	A_α	71.8/4.83	C_α–H_α in β-*O*-4′ substructures (**A**)
	$A_{\beta(G)}$	83.4/4.27	C_β–H_β in β-*O*-4′ substructures (**A**) linked to a G unit
	$A_{\beta(S)}$	85.9/4.10	C_β–H_β in β-*O*-4′ substructures linked (**A**) to a S unit
	B_α	86.8/5.43	C_α–H_α in α-5 phenylcoumaran substructures (**B**)
	C_α	84.8/4.65	C_α–H_α in α–α′ resinol substructures (**C**)
	C_β	53.5/3.05	C_β–H_β in β–β′ resinol substructures (**C**)
	C_γ	71.1/3.81 and 4.16	C_γ–H_γ in β–β′ resinol substructures (**C**)
	D_α	83.5/4.98	C_α–H_α in 5–5′ dibenzodioxocin substructures (**D**)
	E_γ	61.3/4.08	C_γ–H_γ in cinnamyl alcohol end groups (**E**) overlaps with carbohydrate signals
	MeO (-OCH_3)	55.6/3.73	C–H in methoxyls
	X_2'	99.4/4.50	2-*O*-Ac-β-D-Xyl*p*(R)
	X_3'	101.5/4.39	3-*O*-Ac-β-D-Xyl*p*(R)
Aromatic	$H_{2,6}$	127.1/7.17	C_2–H_2 and C_6–H_6 *p*-hydroxyphenyl units (H)
	G_2	110.9/6.99	C_2–H_2 in guaiacyl units (**G**)
	G_5	114.9/6.72 and 6.94	C_5–H_5 in guaiacyl units (**G**)
	G_6	118.7/6.77	C_5–H_5 in guaiacyl units (**G**)
	$S_{2,6}$	103.8/6.69	C_2–H_2 and C_6–H_6 in etherified syringyl units (**S**)
	$pCA_{2,6}$	130.1/7.45	C_2–H_2 and C_6–H_6 in *p*-coumarate (*p*CA)
	$pCA_\beta + FA_\beta$	111.0/7.32	C_2–H_2 in ferulate (FA)
Anomeric	(1–4)-β-D-Glc*p*	102.8/4.40	Cellulose
	D-α-Glc*p*(R)	92.2/5.10	C_α–H_α reducing end of glucose
	D-β-Glc*p*(R)	97.1/4.44	C_β–H_β reducing end of glucose
	(1–4)-β-D-Xyl*p*	102.4/4.50	Xylan
	D-α-Xyl*p*(R)	92.4/5.10	C_α–H_α reducing end of xylose
	D-β-Xyl*p*(R)	97.5/4.38	C_β–H_β reducing end of xylose
	2-*O*-Ac-β-D-Man*p*	98.9/4.86	*O*-2 Acetylated mannan
	3-*O*-Ac-β-D-Man*p*	99.9/4.78	*O*-3 Acetylated mannan

Source: Adapted from Refs [4, 114].

4.11.4 Methoxyl Content Determination

Three selected methods to assess methoxyl contents are described in the following sections.

4.11.4.1 ^{1}H NMR

^{1}H NMR can be used to quantify the methoxyl content. The lignin samples are required to be acetylated before dissolution in $CDCl_3$. The signal for methoxyl protons at ~4.5–3.6 ppm can be quantified [124]. Peak integration is rapid and there is an advantage of a relatively rapid analysis.

4.11.4.2 Hydriodic Acid

In contrast, mixing lignin with the concentrated hydriodic acid (HI) and refluxing [125] can be used to quantify methoxyl content as a wet chemistry method. This method leads to the cleavage of the alkoxyl groups with formation of methyl or ethyl iodide. The volatile iodide, passing through a solution of silver nitrate, yields a precipitate of silver iodide, which is used to determine quantitatively the methoxyl content of the lignin.

4.11.4.3 Direct Methanol

The direct methanol determination has been employed to quantify the methoxyl content [126–128]. In short, lignin is mixed with concentrated sulfuric acid (96% (w/w)). The reaction is exothermic and methanol is formed as a result. Water is added to stop the reaction and methanol is distilled and quantified by GC.

Out of these three methods, ^{1}H NMR method is commonly used because it is simple and does not involve toxic chemicals. The analysis of the resulting NMR spectrum is straightforward. The spectral range and integration region are known.

4.12 Questions for Further Consideration

1. If the actual volume of crystallinity is the same for the cellulose in wood fiber as well as a delignified pulp fiber, will the CrI be equal for the two samples? Will the measurement technique influence this result?
2. After composition analysis of biomass using HPLC your total acid-insoluble lignin mass and monosaccharides adds up to be 91% of the total mass. Explain what other components that may not be accounted for in the total mass.
3. For ^{1}H and ^{31}P NMR analysis of lignin, the total mass of lignin required for analysis is much less than that used in ^{13}C NMR experiments. Why would the same instrument require different concentrations of sample for these different nuclei?
4. Explain why the 2D NMR analysis of lignin is an important breakthrough in the analysis of lignin's structure within wood?

References

1 Resch H, Arganbright DG. Variation of specific gravity, extractive content, and tracheid length in redwood trees. *For Sci.* 1968;**14**(2):148–55.
2 Stefanovic B, Pirker KF, Rosenau T, Potthast A. Effects of tribochemical treatments on the integrity of cellulose. *Carbohydr Polym.* 2014;**111**(0):688–99.

3 Silva GGD, Guilbert S, Rouau X. Successive centrifugal grinding and sieving of wheat straw. *Powder Technol*. 2011;**208**(2):266–70.
4 Kim H, Ralph J. Solution-state 2D NMR of ball-milled plant cell wall gels in DMSO-d6/pyridine-d5. *Org Biomol Chem*. 2010;**8**(3):576–91.
5 Guerra A, Filpponen I, Lucia LA, Argyropoulos DS. Comparative evaluation of three lignin isolation protocols for various wood species. *J Agric Food Chem*. 2006;**54**(26):9696–705.
6 Park S, Johnson DK, Ishizawa CI, Parilla PA, Davis MF. Measuring the crystallinity index of cellulose by solid state ^{13}C nuclear magnetic resonance. *Cellulose (Dordrecht, Neth)*. 2009;**16**(4):641–7.
7 Peng Y, Gardner DJ, Han Y, Kiziltas A, Cai Z, Tshabalala MA. Influence of drying method on the material properties of nanocellulose I: thermostability and crystallinity. *Cellulose (Dordrecht, Neth)*. 2013;**20**(5):2379–92.
8 Jiang F, Hsieh Y-L. Chemically and mechanically isolated nanocellulose and their self-assembled structures. *Carbohydr Polym*. 2013;**95**(1):32–40.
9 Jiang F, Hsieh Y-L. Assembling and redispersibility of rice straw nanocellulose: effect of tert-butanol. *ACS Appl Mater Interfaces*. 2014;**6**(22):20075–84.
10 McCormick CL, Callais PA, Hutchinson Jr, BH. Solution studies of cellulose in lithium chloride and N,N-dimethylacetamide, *Macromolecules* 1985;**18**(12):2394–401.
11 Determination of ash in biomass. Laboratory Analytical Procedure (LAP). [Internet]. 2008.
12 Liu X, Liu Z, Fei B, Cai Z, Jiang Z. Comparative properties of bamboo and rice straw pellets. *BioResources*. 2012;**8**(1):638–47.
13 Determination of structural carbohydrates and lignin in biomass. Laboratory Analytical Procedure (LAP). Available: http://www.nrel.gov/biomass/pdfs/42618.pdf. Accessed 2013 July 7. [Internet]. 2011.
14 Determination of extractives in biomass. http://www.nrel.gov/biomass/pdfs/42619.pdf [Internet]. 2005.
15 Park S, Baker JO, Himmel ME, Parilla PA, Johnson DK. Cellulose crystallinity index: measurement techniques and their impact on interpreting cellulase performance. *Biotechnol Biofuels*. 2010;**3**:10.
16 Park S, Johnson D, Ishizawa C, Parilla P, Davis M. Measuring the crystallinity index of cellulose by solid state 13 C nuclear magnetic resonance. *Cellulose*. 2009;**16**(4):641–7.
17 Sathitsuksanoh N, Zhu Z, Wi S, Zhang Y-HP. Cellulose solvent based biomass pretreatment breaks highly ordered hydrogen bonds in cellulose fibers of switchgrass. *Biotechnol Bioeng*. 2011;**108**(3):521–9.
18 Hurtubise FG, Krässig H. Classification of fine structural characteristics in cellulose by infrared spectroscopy. Use of potassium bromide pellet technique. *Anal Chem*. 1960;**32**(2):177–81.
19 Schultz TP, McGinnis GD, Bertran MS. Estimation of cellulose crystallinity using Fourier transform-infrared spectroscopy and dynamic thermogravimetry. *J Wood Chem Technol*. 1985;**5**(4):543–57.
20 Sun L, Varanasi P, Yang F, Loqué D, Simmons BA, Singh S. Rapid determination of syringyl: guaiacyl ratios using FT-Raman spectroscopy. *Biotechnol Bioeng*. 2012;**109**(3):647–56.

21 Papa G, Varanasi P, Sun L, Cheng G, Stavila V, Holmes B, et al. Exploring the effect of different plant lignin content and composition on ionic liquid pretreatment efficiency and enzymatic saccharification of *Eucalyptus globulus* L. mutants. *Biores Technol*. 2012;**117**:352–9.

22 Lupoi JS, Singh S, Davis M, Lee DJ, Shepherd M, Simmons BA, et al. High-throughput prediction of eucalypt lignin syringyl/guaiacyl content using multivariate analysis: a comparison between mid-infrared, near-infrared, and Raman spectroscopies for model development. *Biotechnol Biofuels*. 2014;**7**(1):93.

23 Rencoret J, Gutiérrez A, Nieto L, Jiménez-Barbero J, Faulds CB, Kim H, et al. Lignin composition and structure in young versus adult *Eucalyptus globulus* plants. *Plant Physiol*. 2011;**115**(2):667–82.

24 Del Rio JC, Rencoret J, Marques G, Li J, Gellerstedt G, Jiménez-Barbero J, et al. Structural characterization of the lignin from jute (*Corchorus capsularis*) fibers. *J Agric Food Chem*. 2009;**57**(21):10271–81.

25 Del Río JC, Marques G, Rencoret J, Martínez ÁT, Gutiérrez A. Occurrence of naturally acetylated lignin units. *J Agric Food Chem*. 2007;**55**(14):5461–8.

26 Del Rio JC, Gutierrez A, Martinez AT. Identifying acetylated lignin units in non-wood fibers using pyrolysis-gas chromatography/mass spectrometry. *Rapid Commun Mass Spectrom*. 2004;**18**(11):1181–5.

27 Cheng K, Sorek H, Zimmermann H, Wemmer DE, Pauly M. Solution-state 2D NMR spectroscopy of plant cell walls enabled by a dimethylsulfoxide-d 6/1-ethyl-3-methylimidazolium acetate solvent. *Anal Chem*. 2013;**85**(6):3213–21.

28 Eudes A, Sathitsuksanoh N, Baidoo EK, George A, Liang Y, Yang F, et al. Expression of a bacterial 3-dehydroshikimate dehydratase reduces lignin content and improves biomass saccharification efficiency. *Plant Biotechnol J*. 2015;**13**(9):1241–50.

29 Eudes A, Zhao N, Sathitsuksanoh N, Baidoo EEK, Lao J, Wang G, et al. Expression of S-adenosylmethionine hydrolase in tissues synthesizing secondary cell walls alters specific methylated cell wall fractions and improves biomass digestibility. *Front Bioeng Biotechnol*. 2016;**4**:doi: 10.3389/fbioe.2016.00058.

30 Wen J-L, Sun S-L, Xue B-L, Sun R-C. Quantitative structural characterization of the lignins from the stem and pith of bamboo (*Phyllostachys pubescens*). *Holzforschung*. 2013;**67**(6):613–27.

31 Martínez ÁT, Rencoret J, Marques G, Gutiérrez A, Ibarra D, Jiménez-Barbero J, et al. Monolignol acylation and lignin structure in some nonwoody plants: a 2D NMR study. *Phytochemistry*. 2008;**69**(16):2831–43.

32 Landucci LL. Quantitative ^{13}C NMR characterization of lignin 1. A methodology for high precision. *Holzforschung*. 1985;**39**(6):355–60.

33 Evtuguin DV, Neto CP, Silva AMS, Domingues PM, Amado FML, Robert D, et al. Comprehensive study on the chemical structure of dioxane lignin from plantation *Eucalyptus globulus* wood. *J Agric Food Chem*. 2001;**49**(9):4252–61.

34 Faix O, Argyropoulos DS, Robert D, Neirinck V. Determination of hydroxyl groups in lignins evaluation of ^{1}H-, ^{13}C-, ^{31}P-NMR, FTIR and wet chemical methods. *Holzforschung*. 1994;**48**(5):387–94.

35 Faix O, Bottcher JH. Determination of phenolic hydroxyl group contents in milled wood lignins by FTIR spectroscopy applying partial least-squares (PLS) and principal components regression (PCR). *Holzforschung*. 1993;**47**(1):45–9.

36 El Mansouri N-E, Salvadó J. Analytical methods for determining functional groups in various technical lignins. *Ind Crops Prod*. 2007;**26**(2):116–24.

37 Mansouri N-EE, Salvadó J. Structural characterization of technical lignins for the production of adhesives: application to lignosulfonate, kraft, soda-anthraquinone, organosolv and ethanol process lignins. *Ind Crops Prod*. 2006;**24**(1):8–16.

38 Kubo S, Kadla JF. Hydrogen bonding in lignin: a Fourier transform infrared model compound study. *Biomacromolecules*. 2005;**6**(5):2815–21.

39 Robert DR, Brunow G. Quantitative estimation of hydroxyl groups in milled wood lignin from spruce and in a dehydrogenation polymer from coniferyl alcohol using ^{13}C NMR spectroscopy. *Holzforschung*. 1984;**38**(2):85–90.

40 Argyropoulos DS, Bolker HI, Heitner C, Archipov Y. ^{31}P NMR spectroscopy in wood chemistry part V. Qualitative analysis of lignin functional groups. *J Wood Chem Technol*. 1993;**13**(2):187–212.

41 El Hage R, Brosse N, Chrusciel L, Sanchez C, Sannigrahi P, Ragauskas A. Characterization of milled wood lignin and ethanol organosolv lignin from miscanthus. *Polym Degrad Stab*. 2009;**94**(10):1632–8.

42 Crestini C, Argyropoulos DS. Structural analysis of wheat straw lignin by quantitative ^{31}P and 2D NMR spectroscopy. The occurrence of ester bonds and α-O-4 substructures. *J Agric Food Chem*. 1997;**45**(4):1212–9.

43 Argyropoulos DS. Quantitative phosphorus-31 NMR analysis of lignins, a new tool for the lignin chemist. *J Wood Chem Technol*. 1994;**14**(1):45–63.

44 Holtman KM, Chang HM, Jameel H, Kadla JF. Quantitative ^{13}C NMR characterization of milled wood lignins isolated by different milling techniques. *J Wood Chem Technol*. 2006;**26**(1):21–34.

45 Kim H, Ralph J, Akiyama T. Solution-state 2D NMR of ball-milled plant cell wall gels in DMSO-d6. *BioEnerg Res*. 2008;**1**(1):56–66.

46 Sathitsuksanoh N, Holtman KM, Yelle DJ, Morgan T, Stavila V, Pelton J, et al. Lignin fate and characterization during ionic liquid biomass pretreatment for renewable chemicals and fuels production. *Green Chem*. 2014;**16**(3):1236–47.

47 Yelle DJ, Kaparaju P, Hunt CG, Hirth K, Kim H, Ralph J, et al. Two-dimensional NMR evidence for cleavage of lignin and Xylan substituents in wheat straw through hydrothermal pretreatment and enzymatic hydrolysis. *Bioenergy Res*. 2013;**6**(1):211–21.

48 Yelle DJ, Ralph J, Frihart CR. Characterization of nonderivatized plant cell walls using high-resolution solution-state NMR spectroscopy. *Magn Reson Chem*. 2008;**46**(6):508–17.

49 Glasser WG, Dave V, Frazier CE. Molecular weight distribution of (semi-) commercial lignin derivatives. *J Wood Chem Technol*. 1993;**13**(4):545–59.

50 Colombini MP, Orlandi M, Modugno F, Tolppa E-L, Sardelli M, Zoia L, et al. Archaeological wood characterisation by PY/GC/MS, GC/MS, NMR and GPC techniques. *Microchem J* 2007;**85**(1):164–73.

51 Tejado A, Pena C, Labidi J, Echeverria JM, Mondragon I. Physico-chemical characterization of lignins from different sources for use in phenol–formaldehyde resin synthesis. *Biores Technol*. 2007;**98**(8):1655–63.

52 Sathitsuksanoh N, Sawant M, Truong Q, Tan J, Canlas CG, Sun N, et al. How alkyl chain length of alcohols affects lignin fractionation and ionic liquid recycle during lignocellulose pretreatment. *BioEnerg Res*. 2015;**8**(3):973–81.

53 Holtman KM, Chang HM, Kadla JF. An NMR comparison of the whole lignin from milled wood, MWL, and REL dissolved by the DMSO/NMI procedure. *J Wood Chem Technol*. 2007;**27**(3–4):179–200.

54 Hatcher PG. Dipolar-dephasing ^{13}C NMR studies of decomposed wood and coalified xylem tissue: evidence for chemical structural changes associated with defunctionalization of lignin structural units during coalification. *Energy Fuels*. 1988;**2**(1):48–58.

55 Park J, Meng J, Lim KH, Rojas OJ, Park S. Transformation of lignocellulosic biomass during torrefaction. *J Anal Appl Pyrolysis* 2013;**100**:199–206.

56 Holtman KM, Chang H-M, Kadla JF. Solution-state nuclear magnetic resonance study of the similarities between milled wood lignin and cellulolytic enzyme lignin. *J Agric Food Chem*. 2004;**52**(4):720–6.

57 Granata A, Argyropoulos DS. 2-Chloro-4, 4, 5, 5-tetramethyl-1, 3, 2-dioxaphospholane, a reagent for the accurate determination of the uncondensed and condensed phenolic moieties in lignins. *J Agric Food Chem*. 1995;**43**(6):1538–44.

58 Ding S-Y, Himmel ME. The maize primary cell wall microfibril: a new model derived from direct visualization. *J Agric Food Chem*. 2006;**54**(3):597–606.

59 Reis D, Vian B. Helicoidal pattern in secondary cell walls and possible role of xylans in their construction. *Comptes Rendus Biologies*. 2004;**327**(9–10):785–90.

60 Balakshin M, Capanema E, Gracz H, Chang H-M, Jameel H. Quantification of lignin–carbohydrate linkages with high-resolution NMR spectroscopy. *Planta*. 2011;**233**(6):1097–110.

61 Determination of protein content in biomass. Laboratory Analytical Procedure (LAP) [Internet]. 2008.

62 Mosse J. Nitrogen-to-protein conversion factor for ten cereals and six legumes or oilseeds. A reappraisal of its definition and determination. Variation according to species and to seed protein content. *J Agric Food Chem*. 1990;**38**(1):18–24.

63 Fengel D, Wegener G. *Wood: chemistry, ultrastructure, reactions*. Walter de Gruyter, Berlin; 1983.

64 Lupoi JS, Singh S, Simmons BA, Henry RJ. Assessment of lignocellulosic biomass using analytical spectroscopy: an evolution to high-throughput techniques. *Bioenerg Res*. 2014;**7**(1):1–23.

65 Lupoi JS, Singh S, Parthasarathi R, Simmons BA, Henry RJ. Recent innovations in analytical methods for the qualitative and quantitative assessment of lignin. *Renew Sustainable Energy Rev*. 2015;**49**:871–906.

66 Teeäär R, Serimaa R, Paakkarl T. Crystallinity of cellulose, as determined by CP/MAS NMR and XRD methods. *Polym Bull*. 1987;**17**(3):231–7.

67 Newman R. Estimation of the lateral dimensions of cellulose crystallites using ^{13}C NMR signal strengths. *Solid State Nucl Magn Reson*. 1999;**15**(1):21–9.

68 Oh S, Yoo D, Shin Y, Seo G. FTIR analysis of cellulose treated with sodium hydroxide and carbon dioxide. *Carbohydr Res*. 2005;**340**(3):417–28.

69 Nelson M, O'Connor R. Relation of certain infrared bands to cellulose crystallinity and crystal latticed type. Part I. Spectra of lattice types I, II, III and of amorphous cellulose. *J Appl Polym Sci*. 1964;**8**(3):1311–24.

70 Nelson M, O'Connor R. Relation of certain infrared bands to cellulose crystallinity and crystal lattice type. Part II. A new infrared ratio for estimation of crystallinity in celluloses I and II. *J Appl Polym Sci*. 1964;**8**(3):1325–41.

71 Segal L, Creely J, Martin Jr, A, Conrad C. An empirical method for estimating the degree of crystallinity of native cellulose using the X-ray diffractometer. *Text Res J*. 1959;**29**(10):786.

72 Ruland W. X-ray determination of crystallinity and diffuse disorder scattering. *Acta Crystallogr*. 1961;**14**(11):1180–5.

73 You C, Chen H, Myung S, Sathitsuksanoh N, Ma H, Zhang XZ, et al. Enzymatic transformation of nonfood biomass to starch. *PNAS*. 2013;**110**(18):7182–7.

74 Wickholm K, Larsson PT, Iversen T. Assignment of non-crystalline forms in cellulose I by CP/MAS ^{13}C NMR spectroscopy. *Carbohydr Res*. 1998;**312**(3):123–9.

75 Silverstein RM, Webster FX, Kiemle D, Bryce DL. *Spectrometric identification of organic compounds*: John Wiley & Sons; 2014.

76 Åkerholm M, Hinterstoisser B, Salmén L. Characterization of the crystalline structure of cellulose using static and dynamic FT-IR spectroscopy. *Carbohydr Res*. 2004;**339**(3):569–78.

77 Kataoka Y, Kondo T. FT-IR microscopic analysis of changing cellulose crystalline structure during wood cell wall formation. *Macromolecules*. 1998;**31**(3):760–4.

78 Nelson ML, O'Connor RT. Relation of certain infrared bands to cellulose crystallinity and crystal latticed type. Part I. Spectra of lattice types I, II, III and of amorphous cellulose. *J Appl Polym Sci*. 1964;**8**(3):1311–24.

79 Li Q, Renneckar S. Supramolecular structure characterization of molecularly thin cellulose I nanoparticles. *Biomacromolecules*. 2011;**12**(3):650–9.

80 Casarano R, Fidale LC, Lucheti CM, Heinze T, Seoud OAE. Expedient, accurate methods for the determination of the degree of substitution of cellulose carboxylic esters: application of UV–vis spectroscopy (dye solvatochromism) and FTIR. *Carbohydr Polym*. 2011;**83**(3):1285–92.

81 Lestander TA, Rhén C. Multivariate NIR spectroscopy models for moisture, ash and calorific content in biofuels using bi-orthogonal partial least squares regression. *Analyst*. 2005;**130**(8):1182–9.

82 Lindgren T, Edlund U, Iversen T. A multivariate characterization of crystal transformations of cellulose. *Cellulose*. 1995;**2**(4):273–88.

83 Kelley S, Rials T, Snell R, Groom L, Sluiter A. Use of near infrared spectroscopy to measure the chemical and mechanical properties of solid wood. *Wood Sci Technol*. 2004;**38**(4):257–76.

84 Eronen P, Österberg M, Jääskeläinen A-S. Effect of alkaline treatment on cellulose supramolecular structure studied with combined confocal Raman spectroscopy and atomic force microscopy. *Cellulose*. 2009;**16**(2):167–78.

85 Gierlinger N, Keplinger T, Harrington M. Imaging of plant cell walls by confocal Raman microscopy. *Nat Protoc*. 2012;**7**(9):1694–708.

86 Agarwal UP. Raman imaging to investigate ultrastructure and composition of plant cell walls: distribution of lignin and cellulose in black spruce wood (*Picea mariana*). *Planta*. 2006;**224**(5):1141–53.

87 Rogošić M, Mencer HJ, Gomzi Z. Polydispersity index and molecular weight distributions of polymers. *Eur Polym J*. 1996;**32**(11):1337–44.

88 Grubisic Z, Rempp P, Benoit H. A universal calibration for gel permeation chromatography. *J Polym Sci B: Polym Lett*. 1967;**5**(9):753–9.

89 Ishii D, Isogai A. The residual amide content of cellulose sequentially solvent-exchanged and then vacuum-dried. *Cellulose (Dordrecht, Neth)*. 2008;**15**(4):547–53.

90 Evans R, Wearne RH, Wallis AF. Molecular weight distribution of cellulose as its tricarbanilate by high performance size exclusion chromatography. *J Appl Polym Sci*. 1989;**37**(12):3291–303.

91 Hiller LA, Jr., Pacsu E. Cellulose studies. V. Reducing end-group estimation. A new method using potassium permanganate. *Text Res J*. 1946;**16**:318–23.

92 Zhang YHP, Lynd LR. Determination of the number-average degree of polymerization of cellodextrins and cellulose with application to enzymatic hydrolysis. *Biomacromolecules*. 2005;**6**(3):1510–5.

93 Kim Y-T, Kim E-H, Cheong C, Williams DL, Kim C-W, Lim S-T. Structural characterization of β-D-(1 → 3, 1 → 6)-linked glucans using NMR spectroscopy. *Carbohydr Res*. 2000;**328**(3):331–41.

94 Johansson M, Samuelson O. Reducing end groups in brich xylan and their alkaline degradation. *Wood Sci Technol*. 1977;**11**(4):251–63.

95 Brown DM, Goubet F, Wong VW, Goodacre R, Stephens E, Dupree P, et al. Comparison of five xylan synthesis mutants reveals new insight into the mechanisms of xylan synthesis. *Plant J*. 2007;**52**(6):1154–68.

96 Peña MJ, Zhong R, Zhou G-K, Richardson EA, O'Neill MA, Darvill AG, et al. Arabidopsis irregular xylem8 and irregular xylem9: implications for the complexity of glucuronoxylan biosynthesis. *Plant Cell*. 2007;**19**(2):549–63.

97 Hatch RS. Cupriethylene diamine as solvent for precise determination of cellulose viscosity. *Ind Eng Chem Anal Ed* 1944;**16**(2):104–7.

98 Gellerstedt G. Gel permeation chromatography. In: Lin SY, Dence CW, editors. *Methods in lignin chemistry*: Springer; 1992. p. 487–97.

99 Chum HL, Johnson DK, Tucker MP, Himmel ME. Some aspects of lignin characterization by high performance size exclusion chromatography using styrene divinylbenzene copolymer gels. *Holzforschung*. 1987;**41**(2):97–108.

100 Majcherczyk A, Hüttermann A. Size-exclusion chromatography of lignin as ion-pair complex. *J Chromatogr A*. 1997;**764**(2):183–91.

101 Contreras S, Gaspar AR, Guerra A, Lucia LA, Argyropoulos DS. Propensity of lignin to associate: light scattering photometry study with native lignins. *Biomacromolecules*. 2008;**9**(12):3362–9.

102 Guerra A, Gaspar AR, Contreras S, Lucia LA, Crestini C, Argyropoulos DS. On the propensity of lignin to associate: a size exclusion chromatography study with lignin derivatives isolated from different plant species. *Phytochemistry*. 2007;**68**(20):2570–83.

103 Glasser WG, Dave V, Frazier CE. Molecular weight distribution of (semi-) commercial lignin derivatives. *J Wood Chem Technol*. 1993;**13**(4):545–59.

104 Robert D. Carbon-13 nuclear magnetic resonance spectrometry. In: Lin SY, Dence CW, editors. *Methods in lignin chemistry*: Springer; 1992. p. 250–73.

105 Björkman A. Studies on finely divided wood. Part 1. Extraction of lignin with neutral solvents. *Svensk Papperstidning – Nordisk Cellulosa*. 1956;**59**(13):477–85.

106 Argyropoulos DS. Quantitative phosphorus-31 NMR analysis of lignins, a new tool for the lignin chemist. *J Wood Chem Technol*. 1994;**14**(1):45–63.

107 Pu Y, Cao S, Ragauskas AJ. Application of quantitative ^{31}P NMR in biomass lignin and biofuel precursors characterization. *Energy Environ Sci*. 2011;**4**(9):3154–66.

108 Zhang W, Sathitsuksanoh N, Simmons BA, Frazier CE, Barone JR, Renneckar S. Revealing the thermal sensitivity of lignin during glycerol thermal processing through structural analysis. *RSC Adv*. 2016;**6**(36):30234–46.

109 Kim H, Ralph J. A gel-state 2D-NMR method for plant cell wall profiling and analysis: a model study with the amorphous cellulose and xylan from ball-milled cotton linters. *RSC Adv*. 2014;**4**(15):7549–60.

110 Rencoret J, Marques G, Gutiérrez A, Nieto L, Santos JI, Jiménez-Barbero J, et al. HSQC-NMR analysis of lignin in woody (*Eucalyptus globulus* and *Picea abies*) and non-woody (*Agave sisalana*) ball-milled plant materials at the gel state. *Holzforschung*. 2009;**63**(6):691–8.

111 Sette M, Lange H, Crestini C. Quantitative HSQC analyses of lignin: a practical comparison. *Comput Struct Biotechnol J*. 2013;**6**(7):1–7.

112 Brandt A, Chen L, van Dongen BE, Welton T, Hallett JP. Structural changes in lignins isolated using an acidic ionic liquid water mixture. *Green Chem*. 2015;**17**(11):5019–34.

113 Sette M, Wechselberger R, Crestini C. Elucidation of lignin structure by quantitative 2D NMR. *Chem Eur J*. 2011;**17**(34):9529–35.

114 Dolan JA, Sathitsuksanoh N, Rodriguez K, Simmons BA, Frazier CE, Renneckar S. Biocomposite adhesion without added resin: understanding the chemistry of the direct conversion of wood into adhesives. *RSC Adv*. 2015;**5**(82):67267–76.

115 Stewart JJ, Akiyama T, Chapple C, Ralph J, Mansfield SD. The effects on lignin structure of overexpression of ferulate 5-hydroxylase in hybrid poplar1. *Plant Physiol*. 2009;**150**(2):621–35.

116 Gille S, de Souza A, Xiong G, Benz M, Cheng K, Schultink A, et al. O-acetylation of Arabidopsis hemicellulose xyloglucan requires AXY4 or AXY4L, proteins with a TBL and DUF231 domain. *Plant Cell*. 2011;**23**(11):4041–53.

117 Yelle DJ, Wei D, Ralph J, Hammel KE. Multidimensional NMR analysis reveals truncated lignin structures in wood decayed by the brown rot basidiomycete *Postia placenta*. *Environ Microbiol*. 2011;**13**(4):1091–100.

118 Bauer S, Sorek H, Mitchell VD, Ibáñez AB, Wemmer DE. Characterization of *Miscanthus giganteus* lignin isolated by ethanol organosolv process under reflux condition. *J Agric Food Chem*. 2012;**60**(33):8203–12.

119 Eichorst SA, Joshua C, Sathitsuksanoh N, Singh S, Simmons BA, Singer SW. Substrate-specific development of thermophilic bacterial consortia by using chemically pretreated switchgrass. *Appl Environ Microbiol*. 2014;**80**(23):7423–32.

120 Yelle DJ, Ralph J, Lu F, Hammel KE. Evidence for cleavage of lignin by a brown rot basidiomycete. *Environ Microbiol*. 2008;**10**(7):1844–9.

121 Shuai L, Yang Q, Zhu J, Lu F, Weimer P, Ralph J, et al. Comparative study of SPORL and dilute-acid pretreatments of spruce for cellulosic ethanol production. *Biores Tech* 2010;**101**:3106–14.

122 Van den Bosch S, Schutyser W, Vanholme R, Driessen T, Koelewijn S-F, Renders T, et al. Reductive lignocellulose fractionation into soluble lignin-derived phenolic

monomers and dimers and processable carbohydrate pulps. *Energy Environ Sci*. 2015;**8**(6):1748–63.

123 Liu Z, Padmanabhan S, Cheng K, Xie H, Gokhale A, Afzal W, et al. Two-step delignification of miscanthus to enhance enzymatic hydrolysis: aqueous ammonia followed by sodium hydroxide and oxidants. *Energy Fuels*. 2014;**28**(1):542–8.

124 Li S, Lundquist K. A new method for the analysis of phenolic groups in lignins by ^{1}H NMR spectroscopy. *Nord Pulp Pap Res J*. 1994;**9**(3):191–5.

125 Chen C-L. Determination of methoxyl groups. In: Lin SY, Dence CW, editors. Methods in lignin chemistry: Springer; 1992. p. 465–72.

126 Balogh D, Curvelo A, De Groote R. Solvent effects on organosolv lignin from *Pinus caribaea* hondurensis. *Holzforschung*. 1992;**46**(4):343–8.

127 Vazquez G, Antorrena G, Gonzalez J, Freire S. FTIR, ^{1}H and ^{13}C NMR characterization of acetosolv-solubilized pine and eucalyptus lignins. *Holzforschung*. 1997;**51**(2):158–66.

128 Ligero P, Villaverde JJ, de Vega A, Bao M. Delignification of *Eucalyptus globulus* saplings in two organosolv systems (formic and acetic acid): preliminary analysis of dissolved lignins. *Ind Crop Prod*. 2008;**27**(1):110–7.